Chemistry & Biology, Vol. 9, 699–706, June, 2002, ©2002 Elsevier Science Ltd. All rights reserved. PII S1074-5521(02)00150-3

Investigation of RNA-Protein and RNA-Metal Ion Interactions by Electron Paramagnetic Resonance Spectroscopy: The HIV TAR-Tat Motif

Thomas E. Edwards, Tamara M. Okonogi, and Snorri Th. Sigurdsson[1]
Department of Chemistry
University of Washington
Seattle, Washington 98195

Summary

Electron paramagnetic resonance (EPR) spectroscopy was used to investigate changes in dynamics of spin-labeled nucleotides in the TAR RNA (U23, U25, U38, and U40) upon binding to cations, argininamide, and two peptides derived from the Tat protein. Nearly identical changes in dynamics were obtained for either calcium or sodium ions, indicating the absence of a calcium-specific structural change for the TAR RNA in solution that had previously been suggested by crystallographic data. Similar dynamic signatures were obtained for two Tat-derived peptides that have the same important binding determinant (R52) and similar binding affinities to the TAR RNA. However, U23 and U38 were substantially less mobile for the wild-type peptide (YGRKKRRQRRR) than for the mutant (YKKKKRK KKKA), demonstrating that, flanking R52, amino acids in the wild-type sequence make specific contacts to the RNA.

Introduction

The interaction between the trans activation-responsive region (TAR) RNA and the Tat protein is required for efficient transcription during replication of the human immunodeficiency virus (HIV) [1–4]. The TAR RNA comprises the first 59 nucleotides on the nascent end of the retrovirus RNA. The Tat binding region in the TAR centers abound a trinucleotide bulge, which is flanked by helical regions (Figure 1A). Nucleotides U23, G26, A27, U38, and C39 have been identified as critical for TAR-Tat binding, and the lower helix has been shown to be an important architectural feature [5, 6]. The loop has been shown to be important for in vivo transcription but is not important for binding of the Tat peptide [5, 7]. Because of its essential role in viral replication, the TAR-Tat interaction is an important drug target.

A combination of biochemical and biophysical experiments has identified the RNA structural changes that occur upon binding to metal ions and derivatives of the Tat protein. The unbound form of the TAR RNA contains a bend of approximately 50° between the lower and upper helices, as observed by transient electric birefringence [8] and NMR [9] (Figure 2A). This bend decreases upon the addition of divalent metal ions [8], allowing the upper and lower duplexes to stack coaxially, as observed in the crystal structure of the TAR RNA [10] (Figure 2B). Although a high-resolution structure of the TAR-Tat complex has not been solved, NMR structures of the RNA component in complexes with structural analogs of Tat have also exhibited coaxial stacking of the duplex regions [11–13]. A characteristic structural feature of the bound TAR RNA is the inversion of the trinucleotide bulge, enabling the formation of a U23•A27•U38 triple base pair (Figure 2C) [14–16].

Although the RNA conformational changes are well understood, not much structural data is available for the Tat protein in the complex. A 10 amino acid-long sequence, G48-R57, in the basic region of the protein is important for TAR-Tat binding [5, 7]. Arginine 52 is essential for the binding, and conservative mutation of flanking residues does not significantly diminish the binding affinity [17]. In fact, an NMR structure of the HIV-2 TAR RNA-argininamide complex [12] has shown how arginine binds to the RNA. Crosslinking experiments have demonstrated the relative proximity of other amino acids to nucleotides in the TAR [18–20] and have been used for modeling of the RNA-peptide complex [21]. However, little is known about the specific interactions between the peptide and the RNA, with the exception of R52.

We are interested in applying electron paramagnetic resonance (EPR) spectroscopy to the study of RNA structure and function, particularly in the context of the TAR-Tat interaction. EPR has been extensively used in the study of proteins, for example to determine conformational changes [22, 23], solvent accessibility at specific sites [24–27], and long-range distances [28, 29]. Although the paramagnetic probe, which is usually a nitroxide spin label, can be conveniently incorporated into proteins by alkylation of cysteine residues, RNA spin labeling has proven to be more challenging. We have recently reported a general method, using readily available materials, for the site-specific incorporation of nitroxide spin labels into internal positions of RNA [30]. This approach relies on the efficient and selective reaction of aliphatic isocyanates with site-specifically incorporated 2′-amino groups in RNA [31] to produce 2′-urea-linked, spin-labeled RNAs (Figure 1C). The spin labels were incorporated into the TAR RNA and were shown to be structurally nonperturbing reporters of motion for the nucleotides to which they were attached [30].

This paper describes the use of EPR spectroscopy to study changes in mobility of four different nucleotides in the TAR RNA upon binding to metal ions, a small molecule, and peptides. Although these experiments do not give direct structural information, the EPR spectra yield a dynamic signature for the binding of a particular compound to the TAR RNA, and this signature was used to distinguish between different RNA binding modes. For example, our experiments indicate that calcium ions present in the crystal structure of the TAR RNA [10] do not induce ion-specific RNA structural changes in solution. As expected, the dynamic signatures of the TAR RNA in the presence of argininamide and two Tat-derived peptides were fairly similar to each other, but different from those observed for the cations. However,

[1]Correspondence: sigurdsson@chem.washington.edu

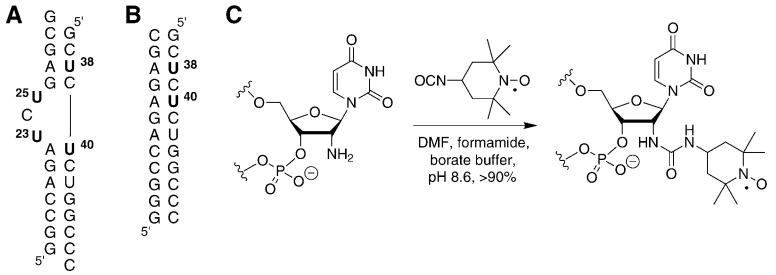

Figure 1. The RNA Sequences Used in this Study and the Spin-Labeling Chemistry

Nucleotides shown in bold were selected for spin labeling.

(A) The TAR RNA construct [10].

(B) An RNA construct lacking the trinucleotide bulge that is essential for Tat binding.

(C) Site-specific spin labeling of RNA with 4-isocyanato TEMPO and 2′-amino-modified RNAs.

the wild-type peptide was shown to induce a significantly larger decrease in the mobility of nucleotides U23 and U38 in the TAR RNA than a mutant peptide with a similar affinity to the RNA, indicating additional RNA-protein contacts.

Results

RNA Spin Labeling and the Effects of Spin Labels on TAR-Tat Binding

Spin-labeled TAR RNAs were prepared with the spin-labeling reagent 4-isocyanato TEMPO, synthesized in one step from 4-amino TEMPO [30], and 2′-amino containing RNAs (Figure 1C). The use of a procedure slightly modified from that previously reported [30] gave up to 2-fold higher yields of purified spin-labeled RNA. Four TAR RNAs, each containing a single spin label at positions U23, U25, U38, or U40, were prepared (Figure 1A). Native polyacrylamide gel electrophoresis (PAGE) was used to determine whether the spin labels interfered with TAR-Tat binding (Figure 3, Table 1). The binding affinity for each of the spin-labeled TAR RNAs was compared to the affinity of the unmodified TAR RNA for two commonly studied Tat-derived peptides, a wild-type (YGRKKRRQRRR) and a mutant (YKKKKRKKKKA) peptide. The equilibrium dissociation constants (K_ds) for the wild-type and mutant peptide upon binding to the unmodified TAR RNA were 0.4 μM and 1.5 μM, respectively. Similar results were obtained for TAR RNAs containing a spin label in positions U23 and U25, whereas an approximately 3-fold lower affinity was observed for U38. In contrast, a larger decrease in binding was observed for U40, but extensive smearing in the gel precluded an accurate determination of its K_ds for binding to the peptides.

EPR Spectroscopy: TAR-Ca^{2+} Binding

Divalent metal ions have been shown to affect the conformation of the TAR RNA [8, 10]. Four calcium ions were present in the crystal structure of the TAR RNA in the absence of Tat (Figure 2B) [10]. To investigate the effect of calcium ions on the TAR RNA in solution, we obtained EPR spectra in the presence and absence of 50 mM $CaCl_2$. EPR spectra of spin-labeled TAR RNAs in the presence of calcium ions showed changes in mobility at U23, U25, U38, and U40 (Figure 4). The greatest change upon addition of calcium ions was observed for U25, for which a moderate increase in the spectral width indicated decreased nucleotide mobility. To test whether this effect was specific for calcium ions, we obtained EPR spectra in the presence of sodium ions at a similar ionic strength (242 mM, including the standard EPR buffer, which contains 92 mM sodium ions). In the presence of sodium ions, all four spin-labeled TAR RNAs showed mobility changes that were nearly identical to those observed in the presence of calcium ions (Figure 4). To determine whether the ionic strength-dependent changes in mobility were specific for the TAR RNA, we repeated this experiment with a duplex construct of the TAR RNA, lacking the trinucleotide bulge that is essential for Tat binding (Figure 1B). A slight change was observed in the spectral width of U38 duplex upon addition of either sodium or calcium ions (our unpublished data). However, this change was signif-

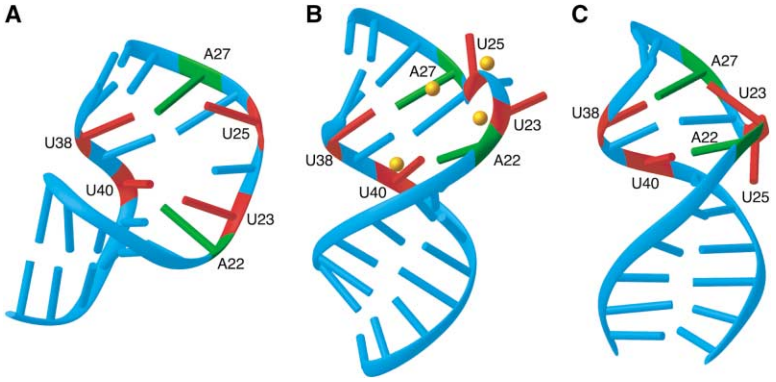

Figure 2. Structures of TAR RNA

The backbone of the TAR RNA is shown in cyan, and spin-labeled residues from this study are shown in red. Residues A22 and A27, which base-pair with residues U40 and U38, respectively, are shown in green.

(A) Solution NMR structure of TAR RNA [9]. The bulge causes a approximately 50° bend between the lower and upper helices.

(B) Crystal structure of the TAR RNA obtained in the presence of calcium ions [10]. The upper and lower duplex regions form a coaxial stack, whereas the bulged residues are pushed out and away from the helix.

(C) NMR solution structure of the HIV-2 TAR RNA bound to argininamide [12]. This structure also reveals a coaxial stack of the helical regions. The bulged residues invert upon binding and allow U23 to form a base triple with U38 and A27.

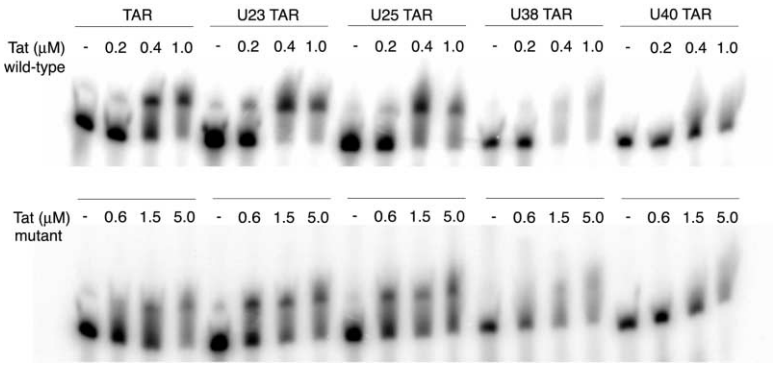

Figure 3. Native PAGE Analysis of TAR-Tat Complex Formation

This analysis was used to determine the equilibrium dissociation constants shown in Table 1.

icantly smaller than that observed for U38 TAR. The change in mobility in the presence of magnesium was also found to be nearly identical to that of calcium and sodium for U23, U38, and U40, whereas U25 became more mobile (our unpublished data).

EPR Spectroscopy: TAR-Argininamide Binding

The solution NMR structure of HIV-2 TAR RNA bound to argininamide [12] provided evidence for the specific interactions of arginine 52 (R52) with the TAR RNA upon binding to the Tat protein. To determine the argininamide binding constant by EPR, we titrated argininamide into a sample of U38 TAR. The spectral width increased up to a 5 mM concentration of argininamide, and we estimated that the U38 TAR-argininamide complex had a K_d of approximately 2–3 mM, similar to the value obtained by NMR (our unpublished data) [12]. EPR spectra of the TAR RNA in the presence of argininamide (5 mM) revealed a small decrease in the mobility of nucleotides U23 and U38 (Figure 5). The mobility of U40 was reduced even more, whereas U25 became more mobile. To investigate if the changes in nucleotide mobility were specific for the TAR RNA, we incubated the duplex lacking the trinucleotide bulge (Figure 1B) with argininamide. We observed virtually no change in the EPR spectra for the U38 or U40 duplex in the presence of argininamide (our unpublished data), demonstrating that the observed changes in mobility for U38 and U40 TAR are specific for the TAR-argininamide complex.

EPR Spectroscopy: TAR-Tat Binding

EPR spectra were obtained for the four different TAR RNAs in the presence of both the mutant (YKKKKRKK KKA) and the wild-type (YGRKKRRQRRR) Tat-derived peptides. To determine the concentration dependence for nonspecific RNA-peptide binding, we titrated the mutant Tat peptide (0.2–2.0 mM) into a sample containing the U38 duplex (Figure 1B) (our unpublished data). We observed virtually no spectral change up to a peptide concentration of 0.5 mM. However, at concentrations above 0.7 mM we observed spectral broadening, combined with multiple spectral features, indicative of nonspecific RNA-protein interactions. These nonspecific interactions have also been observed at this concentration by solution NMR [13]. Thus, the EPR experiments in the presence of the peptides were performed at peptide concentrations of 0.5 mM.

A small decrease in the mobility of U23 and U38 and a moderate decrease in the mobility of U40 (Figure 5) were observed in the presence of the mutant peptide, whereas the mobility of U25 increased (Figure 5). The spectra for U25 and U40 in the presence of the wild-type peptide were similar to that observed for the mutant. In contrast to the results for the mutant peptide, a significant decrease in mobility was observed for nucleotides U23 and U38 in the presence of the wild-type peptide.

Table 1. Equilibrium Dissociation Constants for Peptide Binding to Unmodified and Spin-Labeled TAR RNAs, as Determined by Native PAGE

Spin-Label Site	Tat (wt, μM)	Tat (m, μM)
Unmodified	0.4	1.5
U23	0.3	1.0
U25	0.4	2.0
U38	1.2	5.0
U40	nd	nd

m: mutant; nd: not determined (see text); wt: wild-type

Discussion

Until recently, the application of EPR spectroscopy toward the study of RNA structure and function has been limited to the use of paramagnetic ions to study metal ion binding sites [32–34] because of the lack of efficient and general methods for site-specific incorporation of nitroxide spin labels into RNA. We have recently shown that spin labels can be incorporated into internal, base-paired sites of RNA by conjugation to 2′-amino groups (Figure 1C) [30]. Other spin-labeling strategies include alkylation of sulfur-modified RNA, such as non-base paired 4-thiouridine [35, 36] and terminal [37] or internal phosphorothioates [38], and Pd-catalyzed incorporation of a nitroxide into the 5-position of uridine [39]. Reductive amination has also been used to spin label 3′ ends of RNA [40]. These spin-labeling methods allow incorporation of nitroxide spin labels at several different positions in RNA molecules and thereby facilitate the study of RNA structure and function by EPR spectroscopy.

We have previously shown that the spin labels linked to the 2′-position of U23, U25, U38, and U40 do not appreciably affect the stability of the TAR RNA duplexes [30]. Before utilizing these spin-labeled RNAs for the study of the TAR-Tat interaction by EPR spectroscopy,

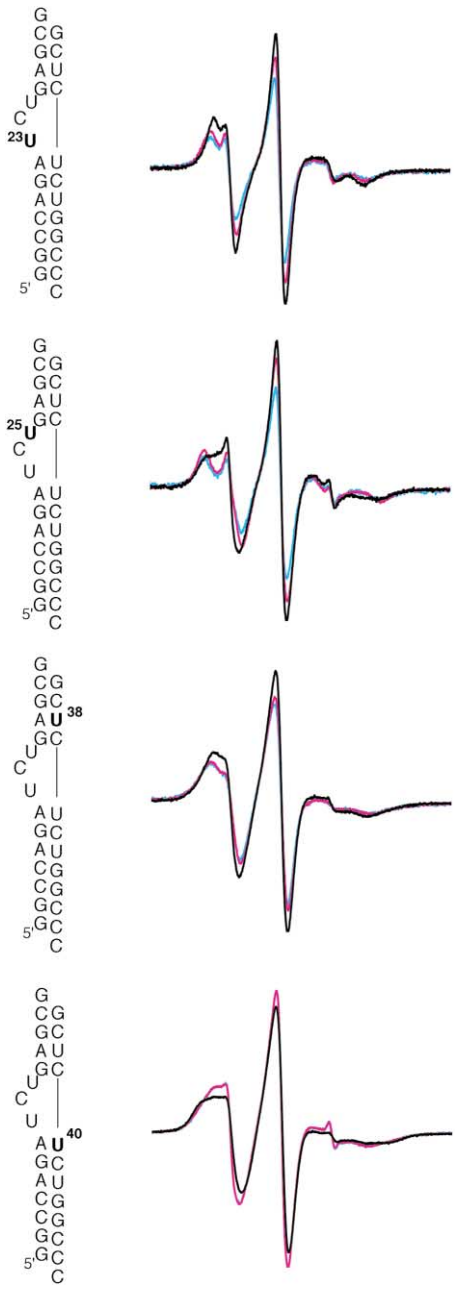

Figure 4. Effect of Metal Ions on the EPR Spectra of TAR RNA

EPR spectra of TAR RNA (black) in the presence of calcium (magenta) or sodium (cyan) ions. The position of the spin label is shown in bold on the RNA to the left of the spectra.

we used native PAGE to determine whether the spin labels affected the stability of the TAR-Tat peptide complex (Figure 3). The equilibrium dissociation constants (K_ds) were determined for both the wild-type (YGR KKRRQRRR) and the mutant (YKKKKRKKKKA) Tat peptides (Table 1). No change in the stability of the TAR-Tat complex was observed for spin labels at positions U23 and U25, whereas the K_ds for U38 were approximately 3-fold lower. On the other hand, a larger decrease was observed for peptide binding to U40. It is not clear why this effect is seen for U40, especially given the fact that the modification is located on the opposite side of the RNA relative to the peptide binding site. Nevertheless, a β-alanyl modification of the 2′ position of U40 has previously been shown to result in a significant decrease in peptide binding, as determined by PAGE [20]. However, the same study revealed a mere 2-fold decrease in binding via filter binding assays [20], which led the authors to propose that the results obtained for the U40 modification by PAGE were due to a high rate of dissociation rather than a low binding constant. We titrated U40 with the wild-type peptide and observed changes in the EPR spectrum until approximately one equivalent of the peptide had been added, after which it did not change more until peptide concentrations above 0.7 mM (our unpublished data). This indicates that U40 binds specifically and stoichiometrically to the peptide under the conditions used for the EPR measurements. We conclude that the spin labels have a small effect on the RNA-peptide binding and that the peptides are fully bound under the conditions used for the EPR spectroscopy.

A crystal structure of the TAR RNA, which was solved in the presence of calcium ions (Figure 2B), revealed three calcium ions concentrated in the bulge region, suggesting that they induce a structural change in the TAR RNA [10]. EPR spectra of the spin-labeled TAR RNAs in the presence of calcium showed a small decrease in mobility, as indicated by increased spectral width, for nucleotides U23, U25, and U38, whereas U40 became more mobile (Figure 4). However, the same change was observed in the presence of sodium ions. Figure 6 shows a quantitative presentation of the data from Figure 4, in which the change in spectral width for each set of conditions is plotted as a function of spin labeled position. This yields a dynamic signature for each compound, and this signature is nearly identical for calcium and sodium ions. Although these results do not constitute a structural proof, they indicate that the conformational change observed upon addition of cations does not require divalent metal ions. Therefore, it is unlikely that divalent metal ions play a specific role in changing the conformation of TAR in the context of TAR-Tat interactions in vivo [10].

Solution NMR studies indicate that argininamide and peptides derived from the Tat protein bind in a similar fashion [11, 12]. Substantial changes were observed in the EPR spectra of the TAR RNA upon addition of argininamide or the peptides (Figure 5), showing that binding affects the mobility of all the spin labeled TAR RNAs. The dynamic signatures for these compounds show the same general features, with the mobility of U23, U38, and U40 decreasing and that of U25 increasing (Figure 6), unlike the results observed for calcium and sodium. The decreased mobility of U23, U38, and U40 is consistent with the current model for the structural change that occurs in the TAR RNA upon binding to Tat [11–13]. In this model, there is a bend between the two helices in the unbound state caused by the trinucleotide bulge (Figure 2A) [8, 9]. Upon binding, the helices stack coaxially, which explains the reduced mobility of U40. Furthermore, the trinucleotide bulge becomes inverted, followed by the formation of a

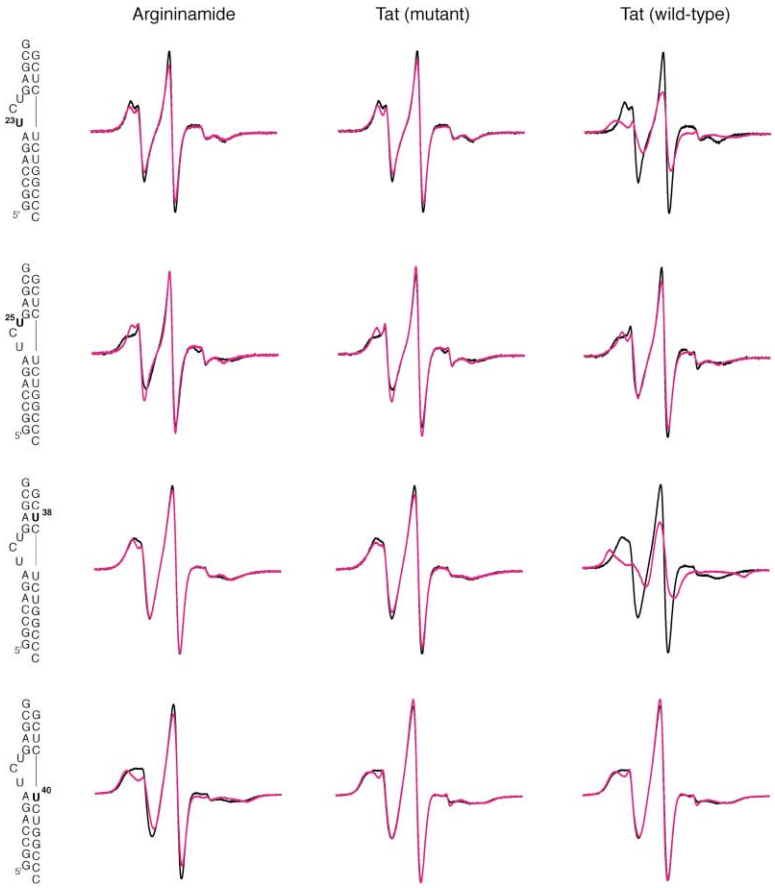

Figure 5. Effect of Tat Derivatives on the EPR Spectra of TAR RNA

EPR spectra of TAR RNA (black) in the presence of argininamide (5 mM) and two Tat-derived peptides (0.5 mM; magenta).

U23•A27•U38 base triple [13, 16] (Figure 2C), resulting in reduced mobility of U23 and U38. In addition, U23 and U38 have been shown to have close contacts with argininamide, which might further reduce their mobility [12].

Although the dynamic signatures for argininamide and the peptides show the same general features, there are dramatic differences in the magnitude of the observed mobility changes. In particular, the EPR data show that the mobilities of U23 and U38 are significantly lower for

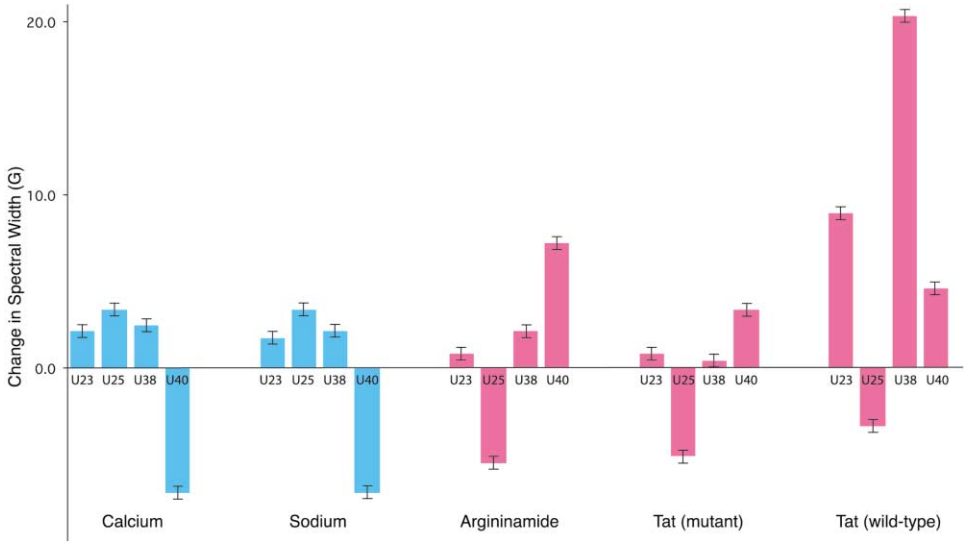

Figure 6. Quantitative Analysis of TAR RNA Binding, yielding a Dynamic Signature for Each Compound Studied

The spectral widths ($2A_{zz}$) were measured between the peaks that flank the central peak and the span from the crest of the low-field peak to the trough of the high-field peak. An increase in spectral width ($\Delta 2A_{zz} > 0$) indicates a decrease in nucleotide mobility.

the wild-type peptide than for the mutant peptide (Figure 6). These data indicate that the two peptides bind differently to the RNA, which is supported by NMR studies of TAR in the presence of mutant peptides for which "the markers for specific complex formation…are largely absent" [13]. This was somewhat unexpected given the fact that the two peptides both contain the essential arginine (R52) and have similar binding affinities to the TAR RNA. Thus, it is clear from our results that other amino acids in the wild-type peptide contribute to the binding specificity, resulting in a more rigid complex in the region of the base triple than was observed for the mutant peptide. On the other hand, argininamide and the mutant peptide have a nearly identical dynamic signature (Figure 6), which indicates that they have a similar mode of binding. The approximately three orders of magnitude-higher binding affinity of TAR to the mutant peptide, relative to argininamide, is presumably caused by a number of electrostatic interactions between positively charged lysine side chains of the peptide and negatively charged RNA phosphodiesters.

Even though we have previously shown that the spin labels used here detect structure-dependent dynamics in the TAR RNA [30], it is possible that some of the EPR data that we attribute to changes in nucleotide dynamics may originate in a mobility change of the spin label, independent of the RNA. For example, direct interactions of the side chains of a peptide with the spin label might reduce its mobility, or a conformational change of a spin-labeled nucleotide could affect the intrinsic mobility of the spin label. However, the data are representative of the expected changes in nucleotide mobility based on the current structural model for the TAR-Tat complex. In addition, by labeling more than one nucleotide in the RNA, we have placed spin labels in a region that is not in direct contact with the peptide, such as at U38. Therefore, it is likely that most of the observed changes in the EPR spectra can be ascribed to changes in nucleotide dynamics.

The EPR results presented here are in agreement with the "induced-fit" rather than the "lock-and-key" theory of RNA-protein binding [41, 42]. Nucleotides (such as U23 and U38) that participate in RNA-protein contacts exhibit significantly more mobility prior to binding. The mobility of nucleotides that do not participate directly in RNA-protein contacts is also affected upon binding. For example, a bulged nucleotide that is not involved in binding (U25) becomes more mobile, whereas an interhelical nucleotide (U40) becomes more rigid as a result of helical stacking. These data show the value of EPR spectroscopy for the study of RNA dynamics in the context of RNA binding to proteins or other molecules.

Significance

Urea-linked spin labels in the 2′ positions of RNA are sensitive probes of nucleotide dynamics. EPR spectra of four TAR RNAs, each containing a spin label in a different position, yielded a dynamic signature for each compound tested. These data were used to evaluate the structural changes in the RNA that occur upon binding to different compounds. For example, the EPR spectra of spin-labeled TAR RNAs in the presence of either sodium or calcium ions were nearly identical, indicating that calcium ions do not induce an ion-specific conformational change of TAR in solution, as suggested by a crystal structure of the TAR RNA. Furthermore, EPR spectroscopy showed that argininamide and the mutant peptide, whose binding constants differ by approximately three orders of magnitude, have similar modes of binding to the TAR RNA. In contrast, the presence of the wild-type peptide, relative to the mutant peptide, dramatically decreased the mobility of U23 and U38. This indicates that, flanking R52, amino acids in the wild-type sequence make specific contacts to the RNA. Because EPR requires small amounts of material (approximately 2 nmol), it will be useful for screening different mutant peptides to determine what other amino acids in the wild-type sequence contribute to the specific binding. This paper represents the first example of using EPR to study changes in RNA dynamics upon peptide binding and shows that EPR spectroscopy is a powerful biophysical technique for the study of RNA interactions with ions, small molecules, and peptides.

Experimental Procedures

Preparation of Spin-Labeled RNAs

Spin-labeling reactions were carried out at −8°C [30]. A solution of crude, deprotected 2′-amino-containing oligonucleotides (Dharmacon Research; 1/4 of a 1 μmol synthesis in 100 μl 70 mM boric acid buffer [pH 8.6]) was treated sequentially with precooled solutions of formamide (60 μl) and 4-isocyanato TEMPO [30] in DMF (75 mM, 40 μl). After 1 hr a second aliquot of 4-isocyanato TEMPO was added. After an additional hour, the solution was washed with $CHCl_3$ (2 × 75 μl), then diluted with sodium acetate (3.0 M, 50 μl [pH 5.3]) and ethanol (−20°C, 1.3 ml). The RNA was precipitated at −20°C over 4 hr, the sample was centrifuged (11,500 rpm, 15 min, 5°C), and the supernatant was removed. The pellet was washed with cold ethanol (2 × 50 μl), dried, dissolved into aqueous urea (8 M, 150 μl), and purified by 20% denaturing PAGE. Samples were quantified with the previously determined molar extinction coefficients [30]. Yields ranged from 100 to 170 nmols, depending on the quality of the RNA synthesis. RNA samples were 5′-^{32}P radiolabeled as described (Gibco BRL) and purified by NAP 25 size exclusion chromatography (Pharmacia).

Purification of Wild-Type Tat-Derived Peptide

Wild-type Tat-derived peptide (YGRKKRRQRRR) was purchased (>95% purity) from United Biochemical Research (Seattle, WA). Samples contained a free-radical contaminant and were purified by G10 Sephadex filtration. A Sephadex G10 column (2.0 g Sephadex) was washed with water (5 ml), and the peptide (306 nmol, 0.43 ODs in 1 ml water; $\epsilon = 1405$, A_{275} single tyrosine) was loaded onto the column and eluted with water. The second 1.0 ml fraction contained most of the peptide (242 nmol, 0.34 ODs) and was shown to be free of the free-spin contaminant by EPR spectroscopy.

Native Gel Shift Assays

TAR RNA samples (2.0 μM RNA in 50 mM sodium cacodylate [pH 6.0]) were annealed on a thermocycler via the following step-wise cooling protocol: 90°C for 2 min, 60°C for 5 min, 50°C for 5 min, 40°C for 5 min, and 22°C for 15 min. The samples were treated with an aqueous solution of the peptide, followed by water up to a final volume of 20 μl (final concentrations: peptide, 0.1–20.0 μM; RNA, 200 nM; buffer, 5.0 mM). Samples were incubated in an ice water bath in a cold room (5°C) for 5 min, diluted with 40% aqueous sucrose (5 μl), and loaded onto a 10% native polyacrylamide gel. The gel was run at 25 mA for 1 hr, dried, and visualized by phosphorimaging.

Equilibrium dissociation constants were determined from between three and eight independent native gels, each of which contained 4–6 protein concentration data points for each RNA. The percentage of bound TAR-Tat complex was determined by densitometry analysis. The percent of bound complex was plotted as a function of Tat concentration with Mac Curve Fit 1.3.3, and the point at which 50% of the complex was bound was estimated to be the K_d. The method of Black et al. [43], which plots [RP]/[R] versus protein concentration, yielded essentially the same result.

EPR Spectroscopy

RNA samples (2.0 nmol in 7.0 μl of 20% aqueous sucrose/100 mM NaCl, 10 mM sodium phosphate, 0.1 mM Na_2EDTA [pH 7.0]) were annealed as described above. Peptide or argininamide (3.0 μl in the above aqueous sucrose buffer; the final concentrations of peptides and argininamide were 0.5 and 5.0 mM, respectively) was added, and the RNA samples (200 μM) were loaded into 0.8 × 1.0 mm quartz capillary tubes (VitroCom). The samples that were used for recording the EPR spectra in the presence of calcium ions (the final concentration was 50 mM, including 2.5 mM magnesium ions) or sodium ions (150 mM increase in concentration; final concentration, 242 mM) were prepared in the same manner. CW-EPR spectra were recorded at 0°C on a Bruker EMX spectrometer with a TE102 cavity. Experimental parameters include 100 KHz modulation frequency, 1.0 G modulation amplitude, 8 mW power, 1024 points, sweep width time of 42 s, sweep width 110 G, and 150–600 scans.

Acknowledgments

We thank Dr. B.H. Robinson for many helpful discussions, Dr. G. Drobny for a gift of the mutant Tat-derived peptide; J.C. Markley, Dr. G. Varani, and the Sigurdsson group for critical review of the manuscript; and the National Institutes of Health (GM56947 and GM62360) for financial support. T.E.E. was supported by National Institutes of Health National Research Service Award 5 T32 GM08268.

Received: October 30, 2001
Revised: April 9, 2002
Accepted: April 10, 2002

References

1. Frankel, A.D. (1992). Activation of HIV transcription by Tat. Curr. Opin. Gen. Dev. *2*, 293–298.
2. Jones, K.A., and Peterlin, B.M. (1994). Control of RNA initiation and elongation at the HIV-1 promoter. Annu. Rev. Biochem. *63*, 717–743.
3. Frankel, A.D., and Young, J.A.T. (1998). HIV-1: fifteen proteins and an RNA. Annu. Rev. Biochem. *67*, 1–25.
4. Frankel, A.D. (2000). Fitting peptides into the RNA world. Curr. Opin. Struct. Biol. *10*, 332–340.
5. Roy, S., Delling, U., Chen, C.H., Rosen, C.A., and Sonenberg, N. (1990). A bulge structure in HIV-1 TAR RNA is required for Tat binding and Tat-mediated *trans*-activation. Genes Dev. *4*, 1365–1373.
6. Weeks, K.M., and Crothers, D.M. (1991). RNA recognition by Tat-derived peptides: interactions in the major groove? Cell *66*, 577–588.
7. Cordingley, M.G., LaFemina, R.L., Callahan, P.L., Condra, J.H., Sardana, V.V., Graham, D.J., Nguyen, T.M., LeGrow, K., Gotlib, L., Schlabach, A.J., et al. (1990). Sequence-specific interaction of Tat protein and Tat peptides with the transactivation-responsive seqenece element of human immunodeficiency virus type 1 *in vitro*. Proc. Natl. Acad. Sci. USA *87*, 8985–8989.
8. Zacharias, M., and Hagerman, P.J. (1995). The bend in RNA created by the trans-activation response element bulge of human immunodeficiency virus is straightened by arginine and by Tat-derived peptide. Proc. Natl. Acad. Sci. USA *92*, 6052–6056.
9. Aboul-ela, F., Karn, J., and Varani, G. (1996). Structure of HIV-1 TAR RNA in the absence of ligands reveals a novel conformation of the trinucleotide bulge. Nucleic Acids Res. *24*, 3974–3981.
10. Ippolito, J.A., and Steitz, T.A. (1998). A 1.3-Å resolution crystal structure of the HIV-1 trans-activation response region RNA stem reveals a metal ion-dependent bulge conformation. Proc. Natl. Acad. Sci. USA *95*, 9819–9824.
11. Aboul-ela, F., Karn, J., and Varani, G. (1995). The structure of the human immunodeficiency virus type-1 TAR RNA reveals principles of RNA recognition by Tat protein. J. Mol. Biol. *253*, 313–332.
12. Brodsky, A.S., and Williamson, J.R. (1997). Solution structure of the HIV-2 TAR-argininamide complex. J. Mol. Biol. *267*, 624–639.
13. Long, K.S., and Crothers, D.M. (1999). Characterization of the solution conformations of unbound and Tat peptide-bound forms of HIV-1 TAR RNA. Biochemistry *38*, 10059–10069.
14. Puglisi, J.D., Chen, L., Frankel, A.D., and Williamson, J.R. (1993). Role of RNA structure in arginine recognition of TAR RNA. Proc. Natl. Acad. Sci. USA *90*, 3680–3684.
15. Tao, J., Chen, L., and Frankel, A.D. (1997). Dissection of the proposed base triple in human immunodeficiency virus TAR RNA indicates the importance of the Hoogsteen interaction. Biochemistry *36*, 3491–3495.
16. Hennig, M., and Williamson, J.R. (2000). Detection of N-H...N hydrogen bonding in RNA via scalar couplings in the absence of observable imino proton resonances. Nucleic Acids Res. *28*, 1585–1593.
17. Calnon, B.J., Tidor, B., Biancalana, S., Hudson, D., and Frankel, A.D. (1991). Arginine-mediated RNA recognition: the arginine fork. Science *252*, 1167–1171.
18. Liu, Y., Wang, Z., and Rana, T.M. (1996). Visualizing a specific contact in the HIV-1 Tat protein fragment and *trans*-activation responsive region RNA complex by photocross-linking. J. Biol. Chem. *271*, 10391–10396.
19. Naryshkin, N.A., Farrow, M.A., Ivanovskaya, M.G., Oretskaya, T.S., Shabarova, Z.A., and Gait, M.J. (1997). Chemical cross-linking of the human immunodeficiency virus type 1 Tat protein to synthetic models of the RNA recognition sequence TAR containing site-specific trisubstituted pyrophosphate analogues. Biochemistry *36*, 3496–3505.
20. Farrow, M.A., Aboul-ela, F., Owen, D., Karpeisky, A., Beigelman, L., and Gait, M.J. (1998). Site-specific cross-linking of amino acids in the basic region of human immunodeficiency virus type 1 Tat peptide to chemically modified TAR RNA duplexes. Biochemistry *37*, 3096–3108.
21. Seewald, M.J., Metzger, A.U., Willbold, D., Rosch, P., and Sticht, H. (1998). Structural model of the HIV-1 Tat(46–58)-TAR complex. J. Biomol. Struct. Dyn. *16*, 683–692.
22. Hubbell, W.L., Gross, A., Langen, R., and Lietzow, M.A. (1998). Recent advances in site-directed spin labeling of proteins. Curr. Opin. Struct. Biol. *8*, 649–656.
23. Hubbell, W.L., Cafiso, D.S., and Altenbach, C. (2000). Identifying conformational changes with site-directed spin labeling. Nat. Struct. Biol. *7*, 735–739.
24. Hubbell, W.L., and Altenbach, C. (1994). Investigation of structure and dynamics in membrane proteins using site-directed spin labeling. Curr. Opin. Struct. Biol. *4*, 566–573.
25. Yu, Y.G., Thorgeirsson, T.E., and Shin, Y.K. (1994). Topology of an amphiphilic mitochondrial signal sequence in the membrane-inserted state: a spin labeling study. Biochemistry *33*, 14221–14226.
26. Lin, Y., Nielsen, R., Murray, D., Hubbell, W.L., Mailer, C., Robinson, B.H., and Gelb, M.H. (1998). Docking phospholipase A2 on membranes using electrostatic potential-modulated spin relaxation magnetic resonance. Science *279*, 1925–1929.
27. Ball, A., Nielsen, R., Gelb, M.H., and Robinson, B.H. (1999). Interfacial membrane docking of cytosolic phospholipase A2 C2 domain using electrostatic potential-modulated spin relaxation magnetic resonance. Proc. Natl. Acad. Sci. USA *96*, 6637–6642.
28. Rabenstein, M.D., and Shin, Y.K. (1995). Determination of the distance between two spin labels attached to a macromolecule. Proc. Natl. Acad. Sci. USA *92*, 8239–8243.
29. Steinhoff, H.J., Radzwill, N., Thevis, W., Lenz, V., Brandenburg, D., Antson, A., Dodson, G., and Wollmer, A. (1997). Determination of interspin distances between spin labels attached to insulin: comparison of electron paramagnetic resonance data with the X-ray structure. Biophys. J. *73*, 3287–3298.
30. Edwards, T.E., Okonogi, T.M., Robinson, B.H., and Sigurdsson,

S.T. (2001). Site-specific incorporation of nitroxide spin-labels into internal sites of the TAR RNA; structure-dependent dynamics of RNA by EPR spectroscopy. J. Am. Chem. Soc. *123*, 1527–1528.

31. Sigurdsson, S.T., and Eckstein, F. (1996). Site specific labelling of sugar residues in oligoribonucleotides: reactions of aliphatic isocyanates with 2′ amino groups. Nucleic Acids Res. *24*, 3129–3133.
32. Horton, T.E., Clardy, D.R., and DeRose, V.J. (1998). Electron paramagnetic resonance spectroscopic measurement of Mn^{2+} binding affinities to the hammerhead ribozyme and correlation with cleavage activity. Biochemistry *37*, 18094–18101.
33. Morrissey, S.R., Horton, T.E., Grant, C.V., Hoogstraten, C.G., Britt, R.D., and DeRose, V.J. (1999). Mn^{2+}-nitrogen interactions in RNA probed by electron spin-echo envelope modulation spectroscopy: application to the hammerhead ribozyme. J. Am. Chem. Soc. *121*, 9215–9218.
34. Morrissey, S.R., Horton, T.E., and DeRose, V.J. (2000). Mn^{2+} sites in the hammerhead ribozyme investigated by EPR and continuous-wave Q-band ENDOR spectroscopies. J. Am. Chem. Soc. *122*, 3473–3481.
35. Hara, H., Horiuchi, T., Saneyoshi, M., and Nishimura, S. (1970). 4-thiouridine-specific spin-labeling of E. coli transfer RNA. Biochem. Biophys. Res. Comm. *38*, 305–311.
36. Ramos, A., and Varani, G. (1998). A new method to detect long-range protein-RNA contacts: NMR detection of electron-proton relaxation induced by nitroxide spin-labeled RNA. J. Am. Chem. Soc. *120*, 10992–10993.
37. Macosko, J.C., Pio, M.S., Tinoco, I., Jr., and Shin, Y.K. (1999). A novel 5′ displacement spin-labeling technique for electron paramagnetic resonance spectroscopy of RNA. RNA *5*, 1158–1166.
38. Qin, P.Z., Butcher, S.E., Feigon, J., and Hubbell, W.L. (2001). Quantitative analysis of the isolated GAAA tetraloop/receptor interaction in solution: a site-directed spin labeling study. Biochemistry *40*, 6929–6936.
39. Strube, T., Schiemann, O., MacMillan, F., Prisner, T., and Engels, J.W. (2001). A new facile method for spin-labeling of oligonucleotides. Nucleosides Nucleotides Nucleic Acids *20*, 1271–1274.
40. Pscheidt, R.H., and Wells, B.D. (1986). Different conformations of the 3′ termini of initiator and elongator transfer ribonucleic acids. J. Biol. Chem. *261*, 7253–7256.
41. Williamson, J.R. (2000). Induced fit in RNA-protein recognition. Nat. Struct. Biol. *7*, 834–837.
42. Leulliot, N., and Varani, G. (2001). Current topics in RNA-protein recognition: control of specificity and biological function through induced fit and conformational capture. Biochemistry *40*, 7947–7956.
43. Black, D.L., Chan, R., Min, H., Wang, J., and Bell, L. (1998). In RNA:Protein Interactions, C.W.J. Smith, ed. (Oxford, UK: Oxford University Press), pp 109–136.